Acta Mech 229, 1567–1577 (2018)
https://doi.org/10.1007/s00707-017-2071-5

ORIGINAL PAPER

MingJun Xu · JiaQing Zhang · ChaoPeng Wu · ChangHai Li · Xiao Chen · ShouXiang Lu

Collision dynamics of a single water droplet impinging on a high-temperature pool of oil

Received: 11 September 2017 / Revised: 28 October 2017 / Published online: 19 December 2017

Abstract The article presents the dynamic process of a single water droplet impinging on a hot oil surface with various temperatures ranging from 205 to 260 °C. Distilled water is used to produce water droplets with different diameters. The impact behavior is recorded by using a high-speed digital camera with the speed of 2000 fps. The result shows that two typical phenomena, including crater–jet–bubble and vapor explosion, can be observed. The vapor explosion occurs when the oil temperature is higher than 210 °C. The oil temperature, the droplet size, and the Weber number are found to have significant influence on the vapor explosion time. The higher the oil pool temperature is, the earlier the vapor explosion occurs. Vapor explosion time increases with the droplet size, while decreases as the droplet Weber number increases. Moreover, the maximum heat absorption for a single water droplet immersing into the hot oil is calculated considering the changes of the droplet size. Both dimensionless maximum crater depth and maximum jet height increase with the pool temperature due to the surface tension, viscous force and decreasing density of the hot oil.

1 Introduction

Cooking oil fire is a relatively common fire accident throughout the world and brings great disasters to mankind [1,2]. According to statistics, 30% of fires were related to kitchen fires in Canada in 1997, and more than 72.6 million dollars had been the cost during the fire accident. In Germany, there were about 200–300 thousands people injured by cooking fire every year. National Fire Protection Association denoted that 30% residential fires were caused by cooking fire [3]. About half of the fire accidents in restaurants, fast food restaurants, and hotels happened in the kitchen [4].

Water spray/mist is widely used in liquid pool fire suppression [5–7] and is proposed to be installed in kitchen [8,9], while its applicability for cooking oil fire needs to be further studied. Although there are many investigations focused on water mist or spray suppressing high-temperature oil fire, the microscopic mechanism is still not clear and quantified [9,10]. Therefore, the topic of droplet impingement has attracted the interest of many researchers [3,11–22]. Liang et al. [11–15] performed systematic experiments on single water droplet impact onto a liquid or solid surface. In particular, they finished a review on single drop impact on a heated wall, which is very helpful to understand the mechanism of single drop interaction with a liquid or solid surface. Zou et al. [16,17] experimentally studied the phenomena of water drop impinging on a restricted liquid surface and stated that the floating, bouncing, coalescence, and splashing can be observed with the increase of Weber number. Gao et al. [18,19] studied the impact behavior of a single drop impacting on a flowing liquid film

M. Xu · C. Wu · C. Li · X. Chen · S. Lu (✉)
State Key Laboratory of Fire Science, University of Science and Technology of China, Hefei 230027, China
E-mail: sxlu@ustc.edu.cn

J. Zhang
State Grid Anhui Electric Power Research Institute, Hefei 230022, China

and solid surface, and on this basis they explored the heat transfer of single drop impact on a film [20]. Additionally, to understand the microscopic mechanism, several researchers have explored the issue using a single droplet from fire suppression perspective. For example, Manzello et al. [3] experimentally studied a water or HFE-7100 droplet impinging onto hot peanut oil. They reported that a vapor explosion occurred when the oil temperature exceeded 220 °C, but the vapor explosion just could be observed when the oil temperature was below 180 °C for a HFE-7100 droplet. However, only peanut oil was used in their experiments, and the falling height and droplet size were not taken into consideration. Lan et al. [21] carried out experiments on a single droplet impacting on a heated alcohol or molten-ghee surface, and stated that the maximum jet height was enlarged and more daughter droplets were splashed for a droplet with additives. Vapor explosion only could be observed for a purified water droplet impinging onto 493 K molten-ghee surface. However, they did not consider the fuel surface with different temperatures. In addition, Wang et al. [22] also performed a series of experiments to explore the dynamic process of a single water droplet with or without additives impinging onto heated molten-ghee surface, and pointed out that the vapor explosion occurred only for a water droplet when the heated surface temperature exceeded 220 °C, i.e., a vapor explosion can be weakened by additives. Also, they did not consider the effects of droplet size and falling height.

In this work, on the basis of previous work described above, a series of experiments on single water droplets with various diameters, which are released from different dropping heights, impacting on heated rapeseed oil are performed. Rapeseed oil is widely used in kitchen, and there are also a lot of fire accidents caused by rapeseed oil which is classified as "K" fire in Standard for Portable Fire Extinguishers (NFPA 10-2007) and Rating and Fire Testing of Fire Extinguishers (UL 711-2004). Understanding the interaction mechanism between water droplet and rapeseed oil has a great significance in the engineering application of water sprinkle/spray/mist.

2 Experimental apparatus and procedures

Figure 1 shows the main experimental setup, including a droplet generator, an injector, a liquid container, a heater device, and a high-speed digital camera with an LED backlighting, which is similar to the apparatus used in previous studies [23,24].

A single water droplet is generated by the injection pump with an injector at a speed of 0.1 ml/h. The droplet is formed at the needle tip and detaches from the syringe due to gravity. The droplet diameter is varied from 2.06 to 3.20 mm by using needles with different sizes. The measuring accuracy is determined by pixel analysis, and the measuring accuracy is ± 0.25 mm. To obtain varied impact Weber numbers, the distance between needle tip and heated surface is changed from 38.6 to 103.3 cm. The impact velocity is calculated by tracking the location of the droplet centroid 1 ms prior to impact, with a measuring accuracy of ± 0.05 m/s. The ambient temperature is fixed at 25 °C. Rapeseed oil is chosen as target liquid and is held by a transparent quartz glass with the size of 75 mm (length) × 75 mm (width) × 80 mm (height). A heater device, which can control the fuel temperature varying from room temperature to 500 °C, is used to heat the rapeseed oil to a specified temperature. Five 0.5-mm-diameter K-type thermocouples with accuracy 0.5 °C, which are located

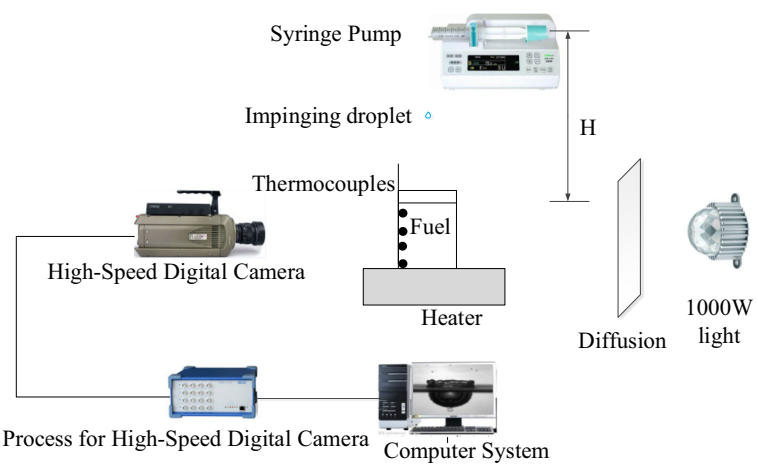

Fig. 1 Schematic diagram of the experimental apparatus

Table 1 Liquid properties

Liquid	Smoke point (°C)	Boiling point (°C)	Density (kg/m^3)
Rapeseed oil	280	310	760
Water	–	–	997

Table 2 Experimental conditions

Droplet diameter (mm)	Impact velocity (m/s)	Weber	Pool temperature (°C)
2.06	3.19	288	205–260
2.06–3.20	3.49	345–543	210, 230
2.06	2.75–4.50	213–571	210

at 1, 3, 6, 20, and 56 mm (pool bottom) beneath the liquid surface are used to monitor the fuel temperature. According to the temperature profile with time, it is found that the temperature varies at most 3 ± 1 °C from the pool bottom to the liquid surface. The dynamical process of a water droplet impacting on a hot surface is recorded by a high-speed digital camera (Phantom V710 with a Nikon 100-mm macrolens) with a speed of 2000 fps and shutter speed of 9 μs. The flicking backlighting consisted of a 1000-W iodine–tungsten light and a thin sheet paper as a diffuser. Tables 1 and 2 show the liquid properties and experimental conditions, respectively. The Weber number is defined as $We = \rho_d v^2 D_0/\sigma$, where ρ_d is the water droplet density, D_0 is the initial droplet diameter, v is the droplet impact velocity, and σ is the droplet surface tension.

3 Results and discussion

3.1 Dynamic process

Although there are many studies focused on a droplet impacting onto a liquid surface [25–32], only a few of them pay attention to the impact behavior of a water droplet impacting on the hot oil with various temperatures. In this work, the pool temperature ranges from 205 to 260 °C. As the pool temperature increases, two typical phenomena, including crater–jet–bubble and vapor explosion, can be observed.

3.1.1 Crater–jet–bubble

Figure 2 shows the evolution process of a single water droplet with diameter of 2.06 mm impacting on a hot oil surface with a temperature of 205 °C. The time when the droplet reaches the surface is set as 0 ms. It should be confirmed that the droplet liquid cannot be dissolved in the rapeseed oil. Similar to the previous studies of a single water droplet impacting onto a hot or burning surface [23,24], as the droplet squeezes the oil, a crater is formed at 22.5 ms and expands outward continuously until the crater reaches its maximum depth. Then all fluid around the crater wall begins to flow inward to fill the crater, and an upward jet forms and rises up continuously until it gets the maximum height at 62.5 ms. After the liquid column collapses, many satellite droplets are formed at the impact point beneath the surface (see Fig. 2, 68 ms). A few hundred milliseconds later, these satellite droplets absorb the heat from the hot oil and evaporate into bubbles (see Fig. 2, 491 ms), and thus it can be deduced that the rising liquid jet may contain a small fraction of water. Additionally, the water droplet penetrates the crater bottom when the crater develops to the maximum depth (see Fig. 2, 22.5 ms) and begins to sink until it reaches the pool bottom at 491 ms. Thus the droplet is heated by the hot oil and pool bottom wall, and then bubbles are intermittently produced from the water droplet, and the droplet size decreases continuously until it disappears. Hence, it is believed that the bubbles are water vapor and the whole water droplet eventually exists in the form of steam. The whole process is named as crater–jet–bubble.

3.1.2 Vapor explosion

When the oil pool temperature is increased to 210 °C, at the initial stage, similar to the former case with pool temperature of 205 °C, the crater and jet can be observed in succession, and also the water droplet penetrates the crater bottom and falls to the pool bottom, as shown in Fig. 3 (595.5 ms). After that, differently from the

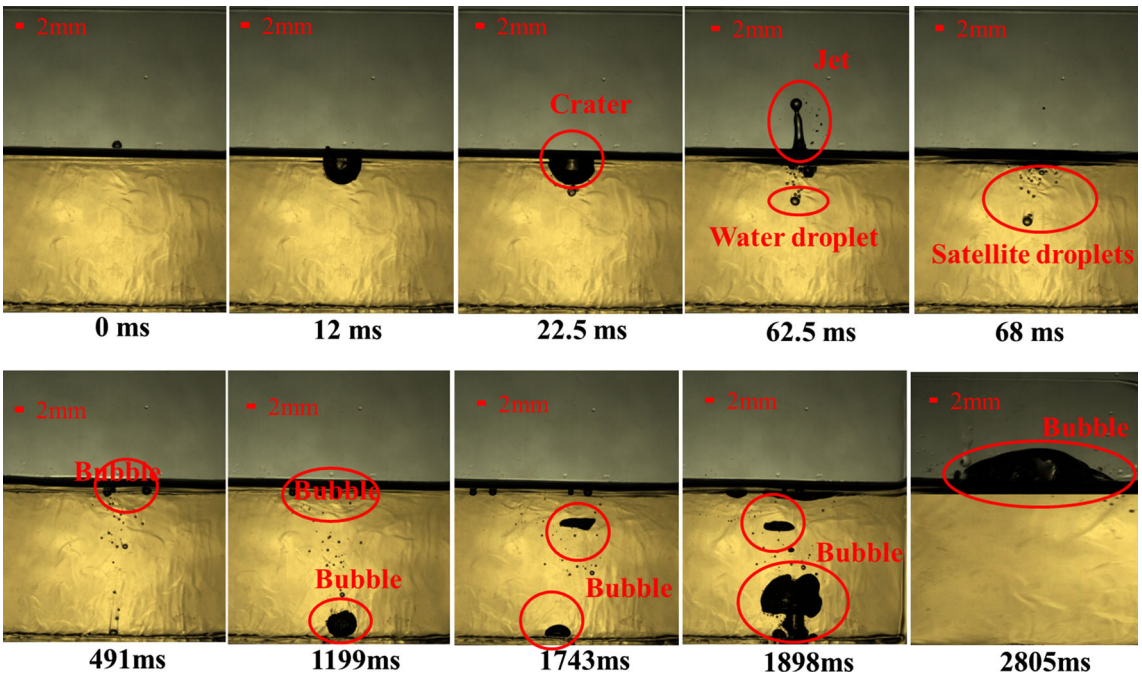

Fig. 2 Dynamic process of single water droplet with diameter of 2.06 mm impacting on 205 °C rapeseed oil pool ($We = 288$)

former case, the droplet volume expands instantaneously from 2286 to 2292 ms and forms a vapor bubble. Then, the parent bubble continues to expand and split into many daughter bubbles. All the bubbles rise to the surface and bring a disturbance to the surface as shown in Fig. 3 (2582 ms). As the oil temperature further increases, the vapor explosion occurs earlier. The quantitative relationship between oil temperature and vapor explosion time will be discussed in a detailed manner hereinafter. As the satellite bubbles move upward, burst occurs on the oil surface finally, which ejects hot oil in any directions. So the intensity of the disturbance is significantly increased by increasing pool temperature, as shown in Fig. 2 (1898 ms), Fig. 3 (2582 ms), and Fig. 4 (1187 ms).

An enlarged view of the formation of vapor bubble is presented in Fig. 5. After the water droplet undergoes a rapid phase transition from liquid to vapor, a vapor bubble is formed, and it expands. But the vapor bubble size experiences an alternate increase and decrease under the effect of external high pressure of surrounding oil and its own expansion force. It can be seen that the radius indicated in Fig. 5 meets the relationship: $r_1 < r_2, r_2 > r_3, r_3 < r_4, r_4 > r_5, r_5 < r_6$. It is a vicious cycle, and the cycle ends until it reaches peak instability: The vapor bubble will eventually rise high enough through the oil to break free of the surface. Meanwhile, the hot oil scatters everywhere accompanyed by a loud pop.

3.1.3 Heat and mass transfer

In the aspect of mass transfer, the mass of droplet liquid is focused. It should be confirmed that the droplet liquid cannot be dissolved in the rapeseed oil. Many satellite water droplets are produced from the parent droplet during the interaction process between parent droplet and hot oil. Then a part of satellite droplets rises to the free surface accompanyed by the oil jet. Another part of the satellite droplets begins to sink since the density of the droplet is larger than the oil's density. All the satellite water droplets absorb the heat from the surrounding hot oil or pool bottom and evaporate into water vapor, i.e., bubbles, and eventually the bubbles rise to the free surface. After the bubble breaks up, the oil pool returns to calm, and only the oil exists in the pool.

In the aspect of heat transfer, we mainly focus on maximum heat absorption. When a single water droplet at room temperature enters into a hot oil pool whose temperature is more than twice of the boiling point of water, the droplet constantly absorbs heat from the surrounding hot oil and pool bottom wall and eventually vaporizes into steam. The whole evaporation process experiences three stages as shown in Fig. 6, including the stage I: the temperature of a water droplet rises from room temperature to 100 °C; the stage II: the 100 °C

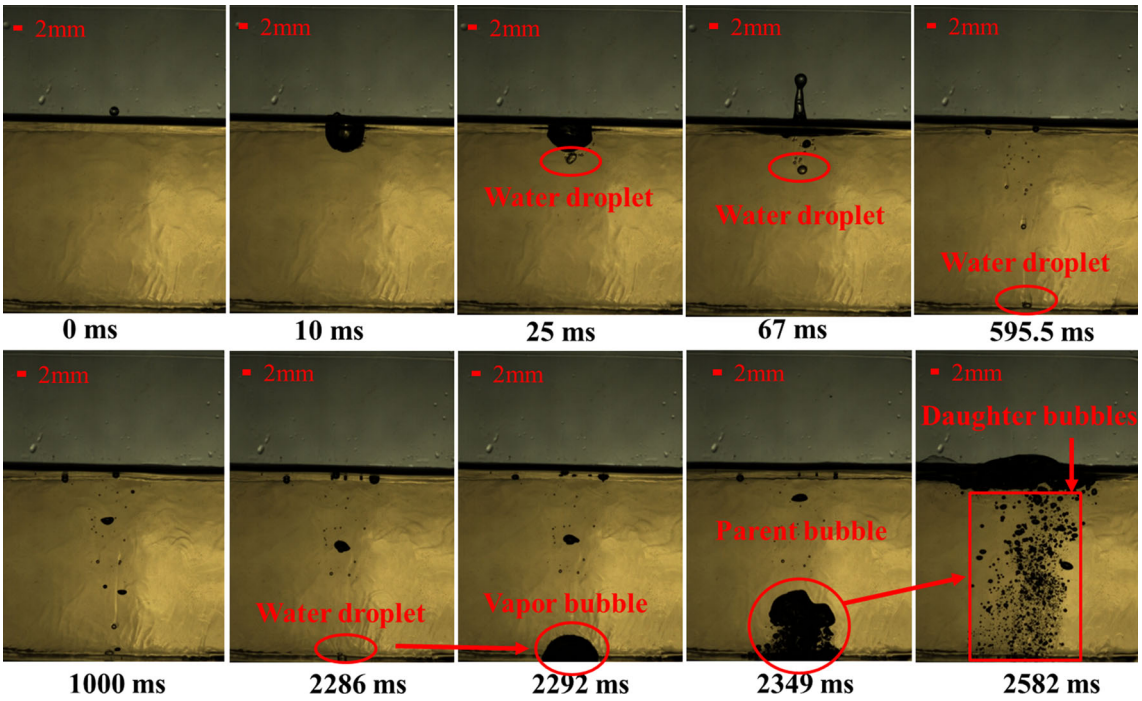

Fig. 3 Dynamic process of water droplet with diameter of 2.06 mm impacting on 210 °C rapeseed oil pool ($We = 288$)

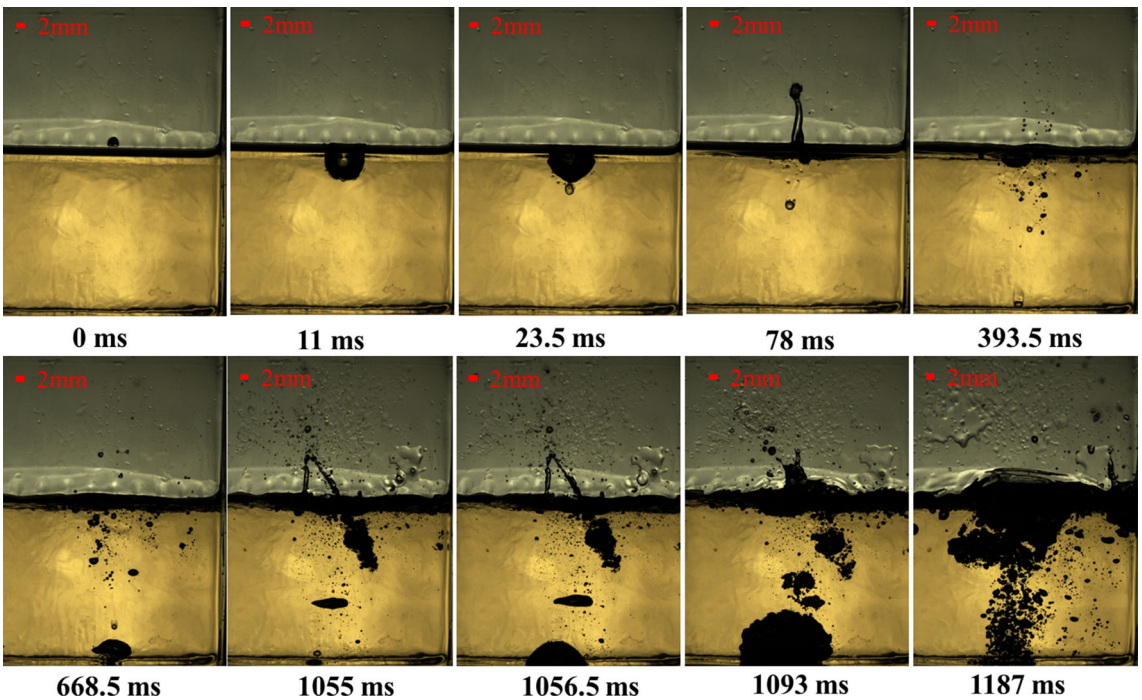

Fig. 4 Dynamic process of a water droplet with diameter of 2.06 mm impacting on a 260 °C rapeseed oil pool ($We = 288$)

water droplet changes from a liquid to water vapor; the stage III: the temperature of vapor rises from 100 °C to the final temperature which is equal to the hot oil temperature.

The heat absorbed by the droplet in stage I, II, and III is calculated by Eqs. (1), (2), and (3), respectively,

$$H_{\mathrm{I}} = m_d C_{p-w} \Delta T_{\mathrm{I}}, \tag{1}$$

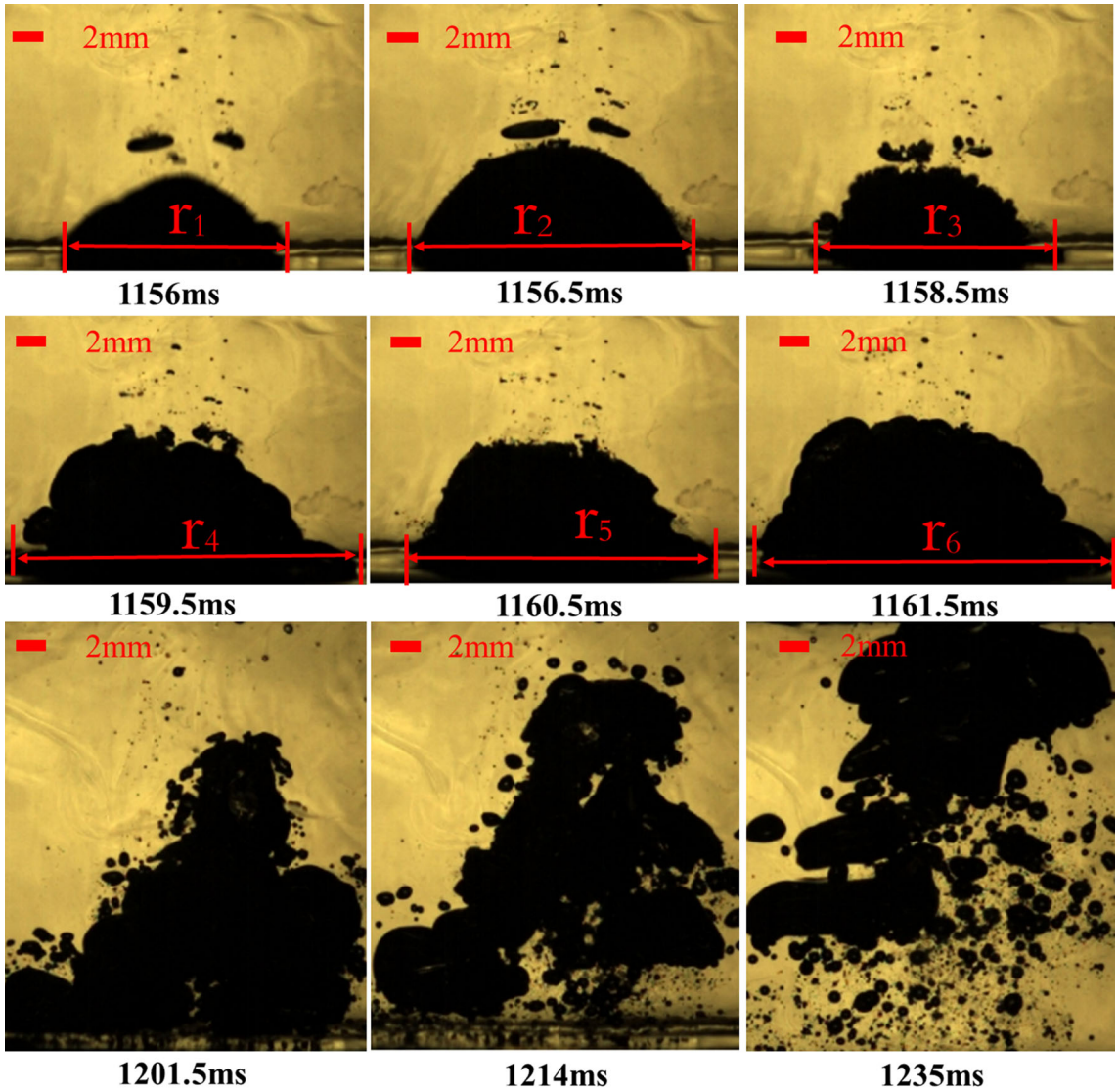

Fig. 5 Enlarged view on the formation of the vapor bubble for 240 °C pool oil ($We = 288$)

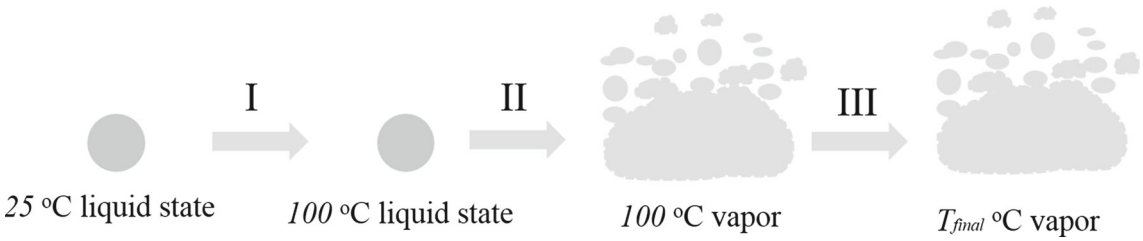

Fig. 6 Evolution process of a single water droplet evaporating into water vapor

$$H_{\mathrm{II}} = m_d \Delta H_w, \tag{2}$$

$$H_{\mathrm{III}} = m_d C_{p-g} \Delta T_{\mathrm{III}} \tag{3}$$

where m_d is the droplet mass, C_{p-w} is the specific heat capacity of liquid water, 4200 J/(kg·°C), ΔT_I is the difference between water boiling point and droplet temperature, ΔH_w is the latent heat of vaporization of water, 2.2572×10^6 J, C_{p-g} is the specific heat capacity of water vapor, 2080 J/(kg·°C), and ΔT_{III} is the difference between final vapor temperature and water boiling point.

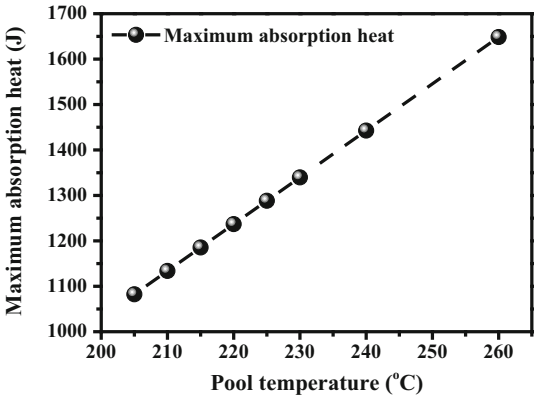

Fig. 7 Maximum absorption heat of single water as a function of pool temperature

Thus, the total heat absorbed in the whole process can be expressed as:

$$H_{\text{total}} = m_d \left(C_{p-w} \Delta T_{\text{I}} + \Delta H_w + C_{p-g} \Delta T_{\text{III}} \right), \tag{4}$$

$$m_d = \rho_d \frac{4\pi}{3} \left(\frac{D_0}{2} \right)^3. \tag{5}$$

Substituting specific data into Eq. (4), the total heat can be calculated:

$$H_{\text{total}} = 10.295 T_{\text{final}} - 1028.1. \tag{6}$$

Figure 7 presents the correlation between pool temperature and maximum absorption heat, as described in Eq. (6). It can be seen that the maximum absorption heat is linearly related to the final water vapor temperature.

3.2 Critical temperature for vapor explosion

Previous investigations have shown that the vapor explosion is determined by the pool temperature [3,22] and suggest that the vapor explosion will occur when the pool temperature is higher than the superheat limit of the cold liquid for liquid–liquid contact. The thermodynamic superheat limit temperature is estimated by Eq. (7) [3,22] for liquid–liquid contact:

$$T_{\text{sl}} = T_{\text{crit}} \left[\left(0.11 \frac{P}{P_{\text{crit}}} \right) + 0.89 \right]. \tag{7}$$

The T_{sl} is the superheat limit temperature of purified water, which can be obtained from [33] 279–302 °C. P is the pressure. T_{crit} and P_{crit} is the critical temperature and critical pressure, respectively. According to Eq. (7), the critical temperature should be approximately equal to the superheat limit temperature in this work. However, both the previous experiments and the present data in this work show that the critical temperature for vapor explosion is below the superheat limit temperature for liquid–solid contact, which may be due to the heat absorbed by the water droplet not only from the pool oil but also from the pool bottom wall. Table 3 shows the critical temperature for a vapor explosion both for present experiments and paper. It is clear that the value in this work is less than the critical temperature both in the studies of Wang and Manzello [3,22]. There is a common disadvantage that the temperature interval is 20 °C both in Wang's and Manzello's studies, so a more detailed temperature value 210 °C is obtained in our work.

3.3 Vapor explosion time

Figure 8 presents the outcomes of the vapor explosion time for different pool temperatures. The cases without vapor explosion are not shown in Fig. 8. It can be found that the explosion time decreases with the pool temperature for both present experiments and papers [22,34]. A higher oil temperature produces a larger temperature difference between droplet and oil, which accelerates the temperature increase in the cold droplet. So the droplet can reach the vapor explosion temperature earlier within an oil pool with a higher temperature.

Table 3 Critical temperature for vapor explosion

Experiments	Droplet	Target liquid	Critical temperature for vapor explosion (°C)
Present	Water	Rapeseed oil	Around 210 °C
Manzello [3]	Water/HFE 7100	Peanut oil	Around 220 °C/140 °C
Wang [22]	Water/5%NaCl/2%AFFF	Molten-ghee	Around 220 °C/220 °C/–

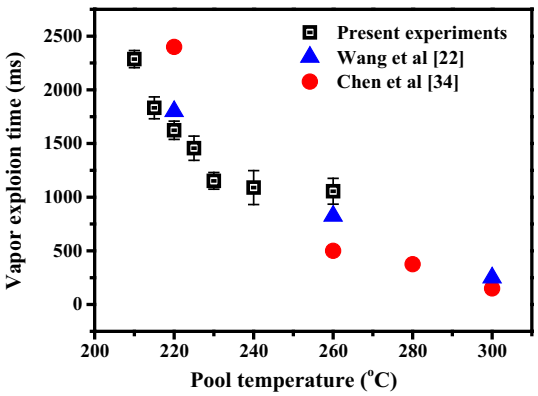

Fig. 8 Vapor explosion time as a function of pool temperature for a fixed droplet size with diameter of 2.06 mm

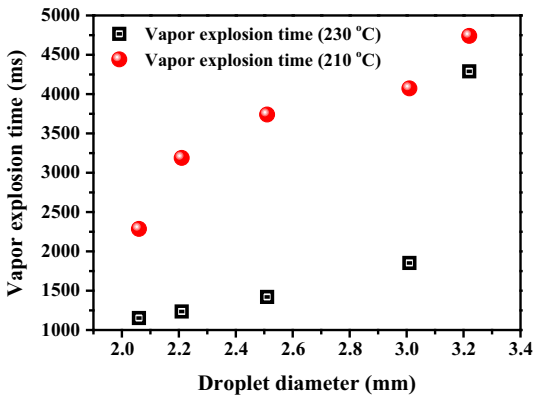

Fig. 9 Vapor explosion time as a function of droplet diameter

3.3.1 Effect of droplet size

In Manzello's study [3], they suppose that the temperature within a smaller droplet of fluid rises faster than within a larger one, and the smaller droplets will reach their critical temperature faster, producing a vapor explosion. Yet, this supposition is not verified in their work since the droplet size is fixed at 3.1 mm in all the experiments. Therefore, to explore the influence of droplet size on the interaction dynamic process, experiments are conducted at fixed pool temperatures with changing droplet diameters. It is obvious that the vapor explosion time increases with the droplet diameter, and the pool temperature also has a significant effect on the vapor explosion time as shown in Fig. 9. Before the water droplet undergoes a phase state transformation, Eq. (8) is used to explain the heat transfer rate between the water droplet with changing diameter and the hot oil with fixed pool temperature. The heat transfer time required to reach the same temperature for a larger droplet may be smaller than that for a smaller droplet. Thus, a smaller droplet can reach the critical temperature of vapor explosion faster,

$$C_{p-w}\frac{\rho_{\mathrm{d}}\pi D_0^3}{6}\frac{\mathrm{d}T}{\mathrm{d}t} = h\pi D_0^2\left(T_{\mathrm{oil}} - T_w\right), \tag{8}$$

where h, T_{oil}, and T_w are heat transfer rate, oil temperature, and droplet temperature, respectively.

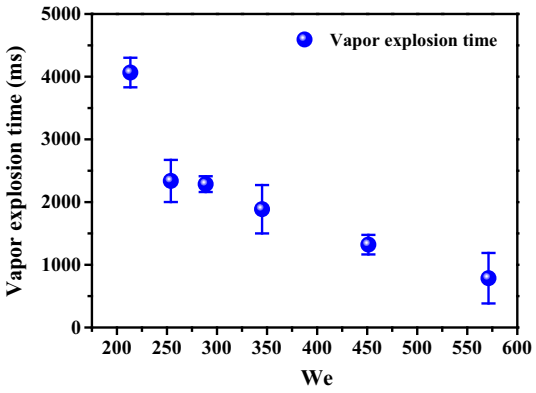

Fig. 10 Vapor explosions as time function of the Weber number for a water droplet with diameter of 2.06 mm impacting on a 210 °C oil pool

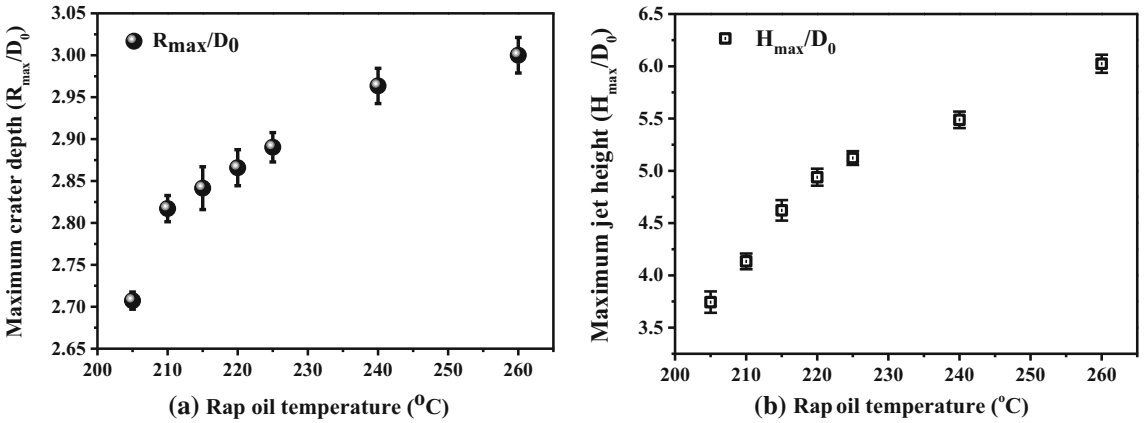

Fig. 11 The maximum crater depth and maximum jet height as functions of rapeseed oil temperature: **a** maximum crater depth; **b** maximum jet height

3.3.2 Effect of the droplet Weber number

Although many studies have focused on the droplet impinging onto hot oil [3,5,22–24], the effects of falling height, i.e., droplet Weber number, were not taken into consideration. In this work, some experiments are performed to explore the effect of the droplet Weber number at a fixed pool temperature, and Fig. 10 displays the influence of the droplet the Weber number on the vapor explosion time. It can be seen that the vapor explosion time increases with the droplet Weber number. This may be caused by two main reasons. Firstly, the impact velocity increases with falling height, which shortens the time of the droplet reaching the pool bottom. The time of the droplet to reach the pool bottom can be obtained from the test video. ($We = 571$, Time = 571 ms; $We = 451$, Time = 610 ms; $We = 345$, Time = 723 ms; $We = 288$, Time = 789 ms; $We = 253$, Time = 900 ms; $We = 213$, Time = 1760 ms). Thus, the droplet can absorb heat not only from oil but also from the pool bottom wall, and the droplet's temperature increases faster. Secondly, a larger falling velocity is favorable for the heat transfer between the droplets and the surrounding hot oil.

3.4 Maximum crater depth and jet height

Figure 11 presents the outcomes of dimensionless maximum crater depth $R_{\max}/D_0$ and maximum liquid jet height $H_{\max}/D_0$ after a single water droplet with fixed Weber number impacting onto a hot pool with different temperatures. It concerns the effects of target liquid physicochemical properties, including surface tension, viscous force and density, and characteristic parameters. The result shows that both the dimensionless maximum crater depth and maximum liquid jet height increase with pool temperature. Since the physicochemical properties of the target liquid are determined by its temperature, the pool temperature increases the surface tension

and viscous force and decreases density, which results in a deeper crater [24]. The deeper crater accumulates more energy, which finally converts to form a higher liquid jet.

4 Conclusions

In this work, a series of experiments were carried out to study the impact behavior, including crater–jet–bubble and vapor explosion, after a single water droplet impacting onto a hot oil pool. The pool temperature ranges from 205 to 260 °C. The vapor explosion occurs when the pool temperature is above 210 °C, and the vapor explosion time decreases with the pool temperature increasing, which is due to a higher oil temperature accelerating the temperature increase in a cold droplet. The correlation between maximum absorption heat of a single water droplet within the hot pool and the droplet diameter is derived. In addition, the droplet size and Weber number have significant effects on the vapor explosion time. The vapor explosion time increases with the droplet size. However, as the droplet Weber number increases, the time of the droplet reaching the pool bottom is shortened, and thus the droplet can absorb heat not only from oil but also from the pool bottom wall. In addition, a larger falling velocity is favorable for the heat transfer between droplet and surrounding hot oil, so the vapor explosion time decreases. Both the dimensionless maximum crater depth and maximum liquid jet height increase with the pool temperature due to the surface tension, viscous force and density of the hot oil decreasing.

Acknowledgements The authors gratefully acknowledge the Fundamental Research Funds for the Central Universities (No. WK2320000034), Class General Financial Grant from the China Postdoctoral Science Foundation (No. 2016M592068), the Fundamental Research Funds for the Central Universities (No. WK2320000037), and the Opening Fund of State Key Laboratory of Fire Science (No. HZ2017-KF06).

References

1. Ahrens, M.: Home Fires Involving Cooking Equipment. National Fire Protection Association, Quincy (2009)
2. Wijayasinghe, M.S., Makey, T.B.: Cooking oil: a home fire hazard in Alberta. Fire Technol. **33**(2), 140–166 (1997)
3. Manzello, S.L., Yang, J.C., Cleary, T.G.: On the interaction of a liquid droplet with a pool of hot cooling oil. Fire Saf. J. **38**, 651–659 (2003)
4. Edwards, N.: A new class of fire. Fire Prev. **310**, 8–8 (1998)
5. Wang, X.S., Zhao, X.D., Zhang, Y., Cai, X., Gu, R., Xu, H.L.: Experimental study on the interaction of a water drop impacting on hot liquid surface. J. Fire Sci. **27**, 545–559 (2009)
6. Cong, B.H., Liao, G.X.: Experimental studies on water mist suppression of liquid fires with and without additives. J. Fire Sci. **27**(2), 101–123 (2009)
7. Cong, B.H., Liao, G., Huang, Z.: Extinguishment of liquid fuel fires by water mist with additives. Fire Saf. Sci. **7**, 95–95 (2007). (In Chinese)
8. Liu, Z., Kim, A.K.: A review of water mist fire suppression technology: part II—application studies. J. Fire. Prot. Eng. **11**(1), 16–42 (2001)
9. Qin, J., Yao, B., Chow, W.K.: Experimental study of suppressing cooking oil fire with water mist using a cone calorimeter. Int. J. Hosp. Manag. **23**(5), 545–556 (2004)
10. Grant, G., Brenton, J., Drysdale, D.: Fire suppression by water sprays. Prog. Energy Combust. Sci. **26**, 79–130 (2000)
11. Liang, G., et al.: Rebound and spreading during a drop impact on wetted cylinders. Exp. Therm. Fluid Sci. **52**, 97–103 (2014)
12. Liang, G., et al.: Experimental investigation of a drop impacting on wetted spheres. Exp. Therm. Fluid Sci. **55**, 150–157 (2014)
13. Liang, G., Mu, X., Guo, Y., et al.: Contact vaporization of an impacting drop on heated surfaces. Exp. Therm. Fluid Sci. **74**, 73–80 (2016)
14. Liang, G., Mu, X., Guo, Y., et al.: Flow and heat transfer during a single drop impact on a liquid film. Numer. Heat Transf. Part B Fundam. **69**(6), 575–582 (2016)
15. Liang, G., Mudawar, I.: Review of drop impact on heated walls. Int. J. Heat Mass Transf. **106**, 103–126 (2017)
16. Zou, J., Ren, Y.L., Ji, C., Ruan, X.D., Fu, X.: Phenomena of a drop impact on a restricted liquid surface. Exp. Therm. Fluid Sci. **51**, 332–341 (2013)
17. Zou, J., Wang, P.F., Zhang, T.R., Fu, X., Ruan, X.: Experimental study of a drop bouncing on a liquid surface. Phys. Fluids **23**(4), 044101 (2011)
18. Gao, X., Li, R.: Spread and recoiling of liquid droplets impacting solid surfaces. AIChE J. **60**(7), 2683–2691 (2014)
19. Gao, X., Li, R.: Impact of a single drop on a flowing liquid film. Phys. Rev. E **92**(5), 053005 (2015)
20. Gao, X., Kong, L., Li, R., et al.: Heat transfer of single drop impact on a film flow cooling a hot surface. Int. J. Heat Mass Transf. **108**, 1068–1077 (2017)
21. Lan, M.J., Wang, X.S., Zhu, P., Chen, P.P.: Experimental study on the dynamic process of a water drop with additives impact upon hot liquid fuel surfaces. Energy Proc. **66**, 173–176 (2015)
22. Wang, Z., et al.: Experimental study on the vapor explosion process of a water drop impact upon hot molten ghee surface. J. Loss Prev. Process. Ind. (2017). https://doi.org/10.1016/j.jlp.2017.03.013

23. Xu, M.J., Wang, C.J., Lu, S.X.: Experimental study of a droplet impacting on a burning fuel liquid surface. Exp. Therm. Fluid Sci. **74**, 347–353 (2016)
24. Xu, M.J., Wang, C.J., Lu, S.X.: Water droplet impacting on burning or unburned liquid pool. Exp. Therm. Fluid Sci. **85**, 313–321 (2017)
25. Liang, G., et al.: Crown behavior and bubble entrainment during a drop impact on a liquid film. Theoret. Comput. Fluid Dyn. **28**(2), 159–170 (2013)
26. Cai, Y.K.: Phenomena of a liquid drop falling to a liquid surface. Exp. Fluids **7**, 388–394 (1989)
27. Liang, G., Mudawar, I.: Review of mass and momentum interactions during drop impact on a liquid film. Int. J. Heat Mass Transf. **101**, 577–599 (2016)
28. Zou, J., Ji, C., Yuan, B.G., Ren, Y.L., Ruan, X.D., Fu, X.: Large bubble entrapment during drop impacts on a restricted liquid surface. Phys. Fluids **24**, 057101 (2012)
29. Rein, M.: Phenomena of liquid drop impact on solid and liquid surfaces. Fluid Dyn. Res. **12**, 61–93 (1993)
30. Thoraval, M.J., Li, Y., Thoroddsen, S.T.: Vortex-ring-induced large bubble entrainment during drop impact. Phys. Rev. E **93**(3), 033128 (2016)
31. Thoraval, M.J., Takehara, K., Etoh, T.G., et al.: von Kármán vortex street within an impacting drop. Phys. Rev. Lett. **108**(26), 264506 (2012)
32. Thoraval, M.J., Takehara, K., Etoh, T.G., Thoroddsen, S.T.: Drop impact entrapment of bubble rings. J. Fluid Mech. **724**, 234–258 (2013)
33. Avedisian, C.T.: The homogeneous nucleation limits of liquids. J. Phys. Chem. Ref. Data **14**(3), 695–729 (1985)
34. Chen, P.P., Wang, X.S., Zhang, Y.: Dynamic process of a water drop impacting onto hot ghee surface. J. Saf. Environ. **11**(6), 213–218 (2011). (In Chinese)